JOURNAL OF APPLIED ELECTROCHEMISTRY 19 (1989) 752–757

Orientation distributions by recovery behaviour in electrodeposited copper layers at room temperature

SV. SURNEV, I. TOMOV

Institute of Physical Chemistry, Bulgarian Academy of Sciences, 1040 Sofia, Bulgaria

Received 15 August 1988

An X-ray diffraction study of the microstructure parameters of the growth and recrystallization texture arising in electrodeposited copper layers at room temperature has been carried out. It was established that the type of recrystallization texture is dependent on the conditions under which the growth texture has been obtained. The orientation distributions of the effective crystallite size, the elastic stored energy and its release rate, which were observed in low-indexed crystal directions, are discussed in connection with the orientation distribution of crystal volumes of the recrystallization texture in the same directions.

1. Introduction

During metal electrodeposition a large number of imperfections form, the quantity of which is commensurable to that in cold worked metals. Such a state is thermodynamically unstable, which is the reason why recovery behaviour, such as recovery and recrystallization, occurs in the metal under suitable conditions.

Recovery processes in electrodeposited copper have been studied by X-ray diffraction both after annealing [1–3] and at room temperature [4]. The papers [1, 5] report on thermally activated recrystallization in thin copper layers. We have shown in previous studies [6, 7] that recovery and recrystallization proceed in electrodeposited copper layers at an observable rate even at room temperature. As a result there were changes in their structure and microhardness.

It is known that defects and grain boundaries in the polycrystalline material are the sites where the excess energy is located – the so-called stored energy [8]. With the help of X-ray diffraction only a part of the total stored energy may be determined – the elastic stored energy. This is linked mainly with the tension fields around dislocations in the bulk of the crystallites.

Assessments of the elastic stored energy in electrodeposited copper have been made in [1, 4]. These studies, however, do not offer any data on the growth and recrystallization textures. An orientation dependence of the elastic stored energy has been observed in the cases of cold-rolled [9, 10] and wire-drawn [11] copper.

Since the stored energy is the driving force of recrystallization, it is to be expected that its orientation distribution in the growth texture is related to the orientation distribution in the recrystallization texture. In this sense the aim of the present study is to obtain information on the link between the orientation distribution in low-indexed directions of the recrystallization texture which has arisen in electrodeposited copper layers at room temperature, and the respective orientation distributions of some structure parameters determinable by X-ray diffraction. To this purpose, with the help of suitable X-ray diffraction methods, we assessed the orientation density, effective crystal size, microdeformations and elastic stored energy, and their change both with cathode current density and time, in specimens prepared at various cathode current densities. At the various current densities, deviating by varying amounts from the equilibrium state, polycrystalline layers were obtained as a result of the different crystallization rates.

2. Specimen preparation and measurement technique

The specimens were electrodeposited copper layers. Their deposition was carried out on rotating brass disc cathodes with a diameter of 32 mm. The cathode rotated at a speed of 80 rpm. The layers were plated in the electrolyte proposed in [12] with the following composition: $CuSO_4 \cdot 5H_2O$ 220 g l^{-1}, H_2SO_4 30 g l^{-1}, NaCl 50 g l^{-1} and brightener agents THB-I and THB-II 3 ml l^{-1}. The temperature of the bath was 25° C. Specimens A, B and C were deposited at cathode current densities, D, of 6, 8 and 10 A dm^{-2}, respectively, with a thickness of $\sim 70\,\mu m$. As standards for the X-ray analysis specimens prepared under the same conditions and annealed for 1 h in vacuum at 500° C were employed.

The X-ray diffraction measurements of the pole figures were carried out with a texture goniometer, reflection scheme [13], CoK_α radiation, Fe filter. The X-ray diffraction line profile was measured by continuous scan with an X-ray diffractometer (Philips, CoK_β radiation, 36 kV, 16 mA, LiF focusing monochromator). The scan speed was 0.5° min^{-1} in the 2θ scale.

0021-891X/89 $03.00 + .12

3. Experimental details

3.1. *Orientation density*

The orientation density gives the frequency with which the fibre axis lies in different crystal directions. By means of diffractometric measurements this density may be determined only in the low-indexed crystal directions, in which it is equivalent to the pole density [14].

To calculate the pole density P_i in the i direction the following known equation was employed [15]:

$$I_i = N_i P_i \tag{1}$$

where I_i is the integrated intensity of the i line, measured with a diffractometer, and N_i is a normalization factor which is calculated from:

$$N_i = N_j(I_i^{rel}/I_j^{rel}) \tag{2}$$

where I_i^{rel} and I_j^{rel} are the theoretically calculated integrated intensities of the relevant diffraction lines i and j. N_j is calculated from Equation 1 after P_j is determined from the relevant pole figure with a texture goniometer according to the method of incompletely measured pole figures of fibre textures [15].

3.2. *Effective crystallite size, microdeformations and elastic stored energy*

The analysis of the broadening of the X-ray diffraction line is a basic method in the study of the structure of polycrystalline materials. The information obtained by it is linked most often with the assessment of the apparent crystallite size and strain. To determine these parameters it is necessary to register at least two orders of reflection hkl. In many practical cases either the higher orders of reflection cannot be measured reliably or there is only a single reflection. There are, however, approximation methods with which it is possible to assess the effective crystallite size and strain from the data of a single line [16]. From the point of view of the strictness of the assumptions and the relatively simple and rapid application the method of Langford *et al.* [17, 18] is to be preferred. This method is based on the assumption [19] that the profile of the X-ray diffraction line may be presented as a convolution of Cauchy and Gaussian functions, namely the Voigt function. The Cauchy (C) and Gaussian (G) components of the integral breadth (integrated intensity divided by the peak intensity) of the experimental (h) and instrumental (g) profiles, may be determined graphically, from the table in [17], or from the empirical formulas derived in [18], in which the integral breadth, β, and full width at half maximum intensity, $2w$, are parameters. The components of the integral breadth of the pure diffraction profile (f) are to be calculated from the expressions:

$$\beta_c^f = \beta_c^h - \beta_c^g \tag{3a}$$

and

$$(\beta_G^f)^2 = (\beta_G^h)^2 - (\beta_G^g)^2 \tag{3b}$$

Under the assumption that the broadening from the apparent crystallite size is only of Cauchy type, while that from the strain, $\tilde{e}$, is only of Gaussian type, D and $\tilde{e}$ are given by

$$D = \lambda/\beta_c^f \cos\theta \tag{4}$$

$$\tilde{e} = \beta_G^f/4 \tan\theta \tag{5}$$

λ and θ being the wavelength and Bragg angle of the diffraction line, respectively.

The elastic stored energy of the crystallites with an $\langle h\,k\,l\rangle$ orientation was assessed by the Faulkner formula, derived under the assumption of an isotropic stress distribution in the deformed material [20]:

$$V_{hkl} = \frac{15E_{hkl}}{2(3 - 4\nu + 8\nu^2)}\langle\tilde{e}^2\rangle \tag{6}$$

where E_{hkl} is Young's modulus in the $\langle hkl\rangle$ direction, ν is Poisson's ratio and $\langle\tilde{e}^2\rangle$ is the mean square microdeformation.

4. Results and discussion

The study on the recovery processes in electrodeposited copper layers was carried out at room temperature.

4.1. *Texture*

The electrodeposited copper platings have a fibre texture. According to the data from the pole figures, the as-fabricated growth texture of the A, B and C specimens consists of a single texture component with $\langle 1\,1\,0\rangle$ orientation. The texture was monitored quantitatively by determining the orientation density, P_{hkl}, in the relevant $\langle h\,k\,l\rangle$ directions. Figure 1a shows the orientation densities P_{hkl} in the $\langle 1\,0\,0\rangle$, $\langle 1\,1\,0\rangle$, $\langle 1\,1\,1\rangle$ and $\langle 3\,1\,1\rangle$ directions for the growth texture of A, B and C (i.e. as a function of D_c). Figure 1b shows the changes which have occurred in P_{hkl} of the investigated $\langle hkl\rangle$ directions after keeping the specimens for 40

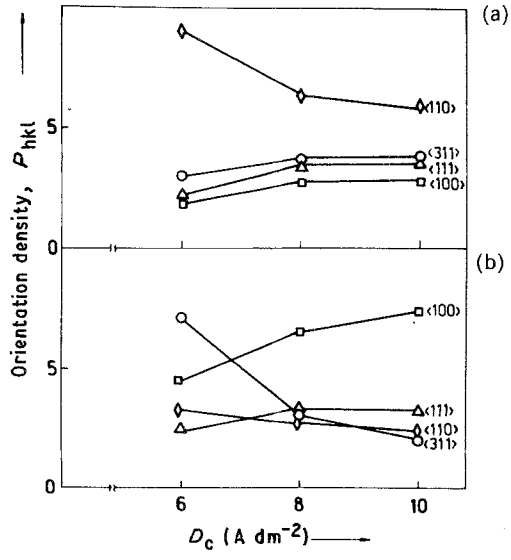

Fig. 1. Plots of the orientation densities, P_{hkl}, of the growth texture (a) and the recrystallization texture (b) vs the current density D_c.

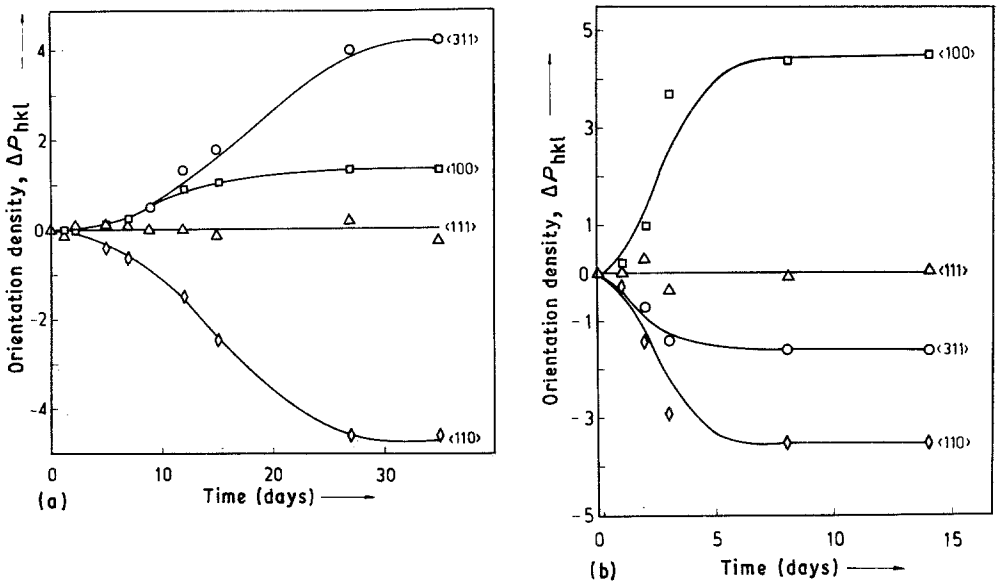

Fig. 2. Plots of the orientation densities, ΔP_{hkl}, vs time: (a) specimen A and (b) specimen C (B).

days at room temperature. We observed structural changes which are analogous to those discussed in earlier studies [6, 7], i.e. this is a case of a process of primary recrystallization occurring at room temperature, as a result of which the copper layer growth texture turns into recrystallization texture. The latter, from the pole figures data, has ⟨3 1 1⟩ + ⟨1 0 0⟩ + ⟨2 2 1⟩ components for the A specimen (⟨2 2 1⟩ is a twin component of the ⟨1 0 0⟩ recrystallization component), while the B and C specimens have very similar recrystallization textures with ⟨1 0 0⟩ + ⟨2 2 1⟩ components. It is evident from Fig. 1 that the substantial changes in these textures take place in the current density, D_c, interval 6–8 A dm^{-2}. What is more, in the specimens obtained at higher cathode current densities the orientation density, P_{110}, of the growth texture is decreased, while P_{100} of the recrystallization texture is increased. An analogous increase in the cube recrystallization texture {1 0 0}⟨1 0 0⟩ with the increase in the amount of cold work has also been observed for rolled copper [21, 22].

Figure 2 presents a close look at the changes of the orientation density, P_{hkl}, vs time in the studied ⟨hkl⟩ directions for the specimens A and C (B is similar to C in its P_{hkl} vs time dependence). For greater clarity we show not P_{hkl}, but their change in relation to their value in the as-fabricated state, i.e.

$$\Delta P_{hkl} = P_{hkl}(\tau) - P_{hkl}(0) \qquad (7)$$

where τ is the time measured in days.

The comparison of Figs 2a (specimen A) and 2b (specimens B and C) reveals the following aspects in the development of the recrystallization texture: (1) the primary recrystallization proceeds at a considerably greater rate in the B and C specimens than in the A specimen – it can be considered finished in B and C on the eighth day, while for A it ends on the 30th day after the electrodeposition; (2) the ⟨3 1 1⟩ component of the recrystallization texture of specimen A increases mainly at the expense of consuming the ⟨1 1 0⟩ component of the growth texture, while the increase of the ⟨1 0 0⟩ component of the recrystallization texture of the B and C specimens is at the expense of the consumption of the ⟨1 1 0⟩ and ⟨3 1 1⟩ components.

It is also evident that the lower the cathode current density for the preparation of a specimen, the later the recrystallization starts, and that the time for the full course of the primary recrystallization is the shortest for the specimen prepared at the highest D_c, under otherwise equal conditions.

4.2. *Effective crystallite size and strains*

The next step in our study is concerned with obtaining information on the specimen microstructure from the profile analysis of the X-ray diffraction lines.

Table 1 lists the results for the effective crystallite size, D_{hkl}, the strains, $\tilde{e}_{hkl}$, and the elastic stored energy, V_{hkl}, determined in the as-fabricated state.

Table 1. The effective crystallite size D, *strains* ẽ *and elastic stored energy* V *in the ⟨1 1 1⟩, ⟨1 0 0⟩, ⟨1 1 0⟩ and ⟨3 1 1⟩ directions for the A, B and C specimens measured in the as-fabricated state*

⟨hkl⟩	D (Å)			ẽ × 10^3			V (cal g atom^{-1})		
	A	*B*	*C*	*A*	*B*	*C*	*A*	*B*	*C*
1 1 1	342 ± 88	307 ± 36	315 ± 50	1.3 ± 0.2	1.4 ± 0.2	1.3 ± 0.2	1.6 ± 0.4	1.8 ± 0.4	1.6 ± 0.4
1 0 0	171 ± 20	174 ± 20	174 ± 29	3.6 ± 0.3	4.4 ± 0.3	4.2 ± 0.3	4.3 ± 0.7	6.4 ± 0.8	5.8 ± 0.7
1 1 0	387 ± 90	460 ± 103	400 ± 98	2.3 ± 0.2	3.1 ± 0.2	3.0 ± 0.2	3.4 ± 0.5	6.1 ± 0.5	5.7 ± 0.5
3 1 1	183 ± 13	207 ± 36	171 ± 29	2.1 ± 0.2	2.7 ± 0.2	2.4 ± 0.3	2.1 ± 0.4	3.4 ± 0.5	2.7 ± 0.6

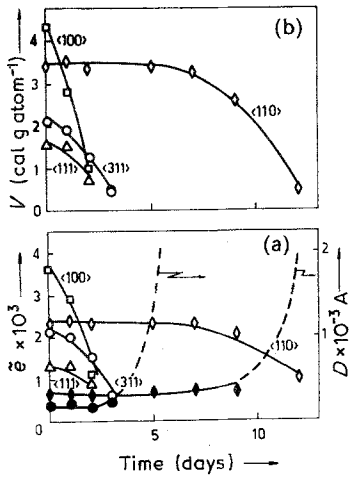

Fig. 3. Plots of the strains, $\tilde{e}$, (a) effective crystallite size, D, and elastic stored energy, V, in cal g atom^{-1} (b) vs time in days.

These results indicate that the crystallite size in a given ⟨hkl⟩ direction remains constant within the error limits for the various specimens. It is largest in the ⟨1 1 0⟩ and ⟨1 1 1⟩ directions, and considerably smaller in the ⟨1 0 0⟩ and ⟨3 1 1⟩ directions, i.e. there is an orientation distribution of the effective crystallite size.

With the increase in the current density the values of the strain (resp. the elastic energy) increase in the crystallites with ⟨1 0 0⟩ and ⟨1 1 0⟩ orientation, while in the ⟨1 1 1⟩ and ⟨3 1 1⟩ directions they remain constant within the error limits.

Data on the effective crystallite size and strains for the time following the electrodeposition have been registered only for the A specimen. It was impossible to obtain such for B and C since their values for the effective crystallite size and strain were outside the range of reliable determination on the very next day after deposition, i.e. $D_{max} > 1500$ Å and $\tilde{e}_{min} < 2 \times 10^{-4}$, respectively.

Figure 3 shows the change in the strain and the effective crystallite size (a) and in the elastic stored energy (b) for the A specimens vs time. It can be seen that in the ⟨1 0 0⟩, ⟨1 1 1⟩ and ⟨3 1 1⟩ directions the strain falls under its minimum measurable value, $\tilde{e}_{min}$, during the first 2–3 days after the electrodeposition, while the effective crystallite size remains constant (within the error limits). Consequently, the decrease in the strain (resp. the release of the elastic stored energy) during the first 2–3 days may be linked to the occurrence of a recovery process. This is also confirmed by the absence of any changes in the texture for the same time interval. Immediately afterwards the crystallite size increases considerably, exceeding the maximum measurable value, D_{max}, due to a primary recrystallization in the relevant crystal directions (an idea for the evolution of the crystallite size vs time is shown for the ⟨3 1 1⟩ direction). Analogous changes in the microstructure in the direction of the main component of the growth texture, ⟨1 1 0⟩, begin to be observed only 10–12 days after the layer is prepared. Consequently the release of the elastic stored energy, V_{110}, occurs at a considerably slower rate than in the other three directions.

The following inequalities are valid for the values of the elastic stored energy for the A, B and specimens in the as-fabricated state:

$$V_{100} \gtrsim V_{110} > V_{311} > V_{111} \qquad (8)$$

i.e. there is an orientation distribution of V_{hkl} in the specimens. Some authors [23–25] have established, for low carbon steel sheets, that in the directions in which the elastic stored energy is the highest, the recrystallization proceeds at a higher rate than in those with a lower energy. In the case of the present copper layers, by comparing the inequalities (8) with the change in the pole densities in the relevant ⟨hkl⟩ direction vs time (Fig. 2), we observe that a similar dependence does not hold at all. For example, the high value of the elastic stored energy in the ⟨1 1 0⟩ direction cannot be linked to the disappearance of the respective component in the recrystallization texture, and the low value of V_{311} – to the arising of the main recrystallization component of the A specimen – ⟨3 1 1⟩. What is more, the inequalities (8) are valid for the A, B and C specimens at the same time, while their recrystallization textures differ from one another. Moreover, in recent studies of low carbon steel sheets [26, 27] similar discrepancies with the dependence of the distribution of the elastic stored energy on the recrystallization rate in the relevant crystal directions established in [23–25] have been noted. It is evident that the knowledge of the orientation distribution of the elastic stored energy in the growth texture is not sufficient to explain the reasons for the type of recrystallization texture.

For the above reasons, the experimental data presented so far on the microstructural changes with time are relevant only for one of the specimens (A). This required the pure integral breadth of the X-ray diffraction lines to be used for characterizing the structural changes in the three specimens. The change in the integral breadth vs time yields a qualitative idea of the recovery behaviour. This is so, since the effects of the apparent crystallite size and strains which are sensitive as regards the recovery behaviour, contribute to the integral line breadth. Figure 4 presents the change of the pure integral breadths*, β, vs time, τ, for the A and C specimens. The dependence, $\beta(\tau)$, for specimen B duplicates that of specimen C. The integratal breadths, β_{hkl}, of the hkl lines are normalized to 1 as regards their respective values measured in the as-fabricated state. An analogous presentation of $\beta(\tau)$ for the processes of recovery and recrystallization has been employed in [5].

With the purpose of assessing the recovery behaviour in the various crystal directions we defined the parameter recovery rate of the diffraction line breadth R. We adopted its numerical value to be equal to the reciprocal value of the time, $\tau_{0.5}$, during which τ

* β was calculated according to the formula: $\beta = B - b^2/B$ [28], where B is the observed line breadth and b is its instrumental breadth.

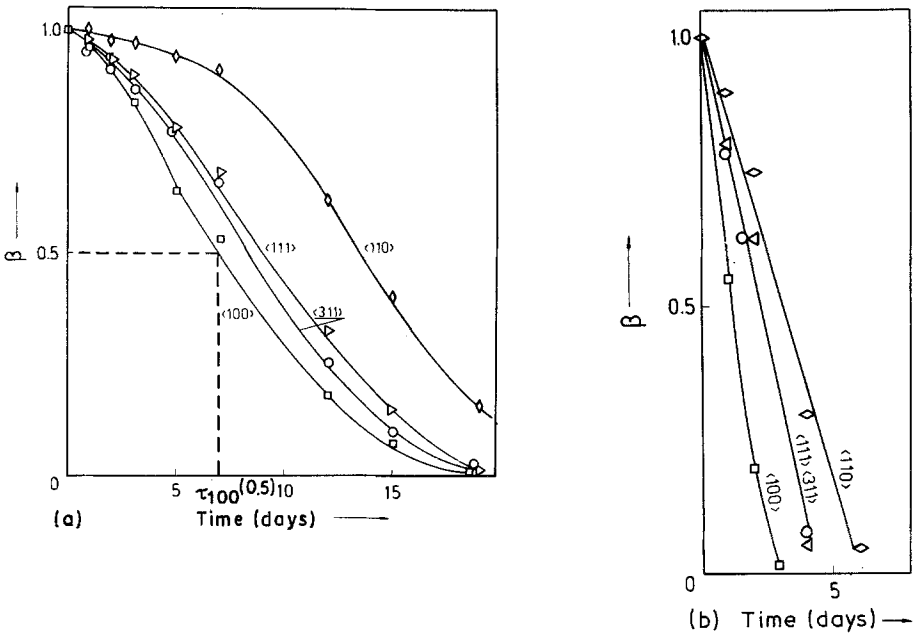

Fig. 4. Plots of the pure integral breadths, β, normalized to 1 as regards their value in the as-fabricated state, vs time: (a) specimen A and (b) specimen C (B).

decreases by a factor of two. Figure 4a shows an example of the determination of the time $\tau_{100}(0.5)$ for a twofold decrease of the integral breadth of the line 200.

It becomes evident from Fig. 4 that the rate of decrease of the integral breadths, β_{hkl}, for the B and C specimens is considerably greater than that for the A specimen. Moreover, it differs in the various ⟨hkl⟩ directions. For all specimens studied, the following inequalities hold:

$$R_{100} > R_{311} \gtrsim R_{111} > R_{110} \qquad (9)$$

This signifies that the orientation distribution of the recovery rates of the integral breadths is analogous for the three specimens.

Essentially the rate of decrease of the pure integral breadth, R_{hkl}, depends specifically on the respective increase of the crystallite size, D_{hkl} (resp. the release of the stored energy of the grain boundaries), and on the decrease of the strains, $\tilde{e}_{hkl}$ (resp. the release of the elastic stored energy, V_{hkl}). The distinct course of this dependence is unknown, but the orientation distribution of R_{hkl} gives a qualitative idea of the sum total rate of these two types of stored energy in the various ⟨hkl⟩ crystal directions. It has been established, in the case of cold worked metals, that the ratio of elastic stored energy and stored energy of the grain boundaries is strongly in favour of the latter [8]. This would cause an undoubtedly dominating effect on the part of the stored energy of the grain boundaries on the type of recrystallization texture. In this sense the established dependence (9) between the rates of decrease of the integral breadths, R_{hkl}, concurs better with the observed orientation distribution in the recrystallization texture than the orientation distribution (8).

4.3. *Microhardness*

Figure 5 shows the change of the Vickers hardness HV vs time for the A and B specimens (C has an analogous course for HV as B). There is a correspondence in the decrease of the microhardness both with the rate of the change of the integral breadth and the observed texture changes.

5. Conclusions

In connection with the orientation distribution of the crystal volumes in the recrystallization texture, arising in copper layers at room temperature, we investigated the effect of the cathode current density, D_c, on both the growth texture and the changes of the effective crystallite size and their microdeformations.

We established that: (i) the specimens prepared at higher current, D_c, have a lower sharpness of the only component of the growth texture ⟨1 1 0⟩, and have an increased strain (resp. elastic stored energy) in the same component; (ii) the type of recrystallization texture depends on the growth texture preparation conditions: at low D_c a recrystallization texture ⟨3 1 1⟩ + ⟨1 0 0⟩ + ⟨2 2 1⟩ is obtained, while at high D_c, a sharp ⟨1 0 0⟩ + ⟨2 2 1⟩; (iii) there is an

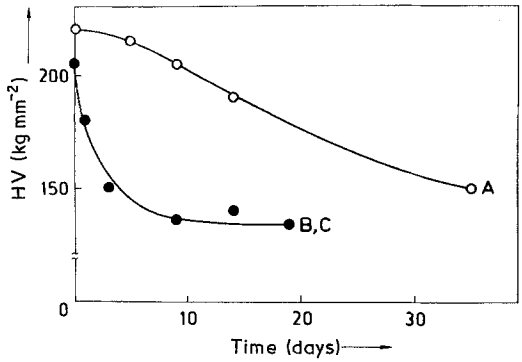

Fig. 5. Plots of the Vickers microhardness, HV, in kg mm^{-1} vs time in days, for the A specimen (○) and B (C) (●), respectively.

orientational distribution of the effective crystallite size of the stored energy and of the rate of its release.

Acknowledgement

The authors would like to express their gratitude to Dr D. Stoychev for placing at their disposal the electrolyte in which the specimens were prepared.

References

[1] E. M. Hofer and H. E. Hintermann, *J. Electrochem. Soc.* **112** (1965) 167.
[2] A. Gangulee, *J. Appl. Phys.* **43** (1972) 867.
[3] A. Gangulee, *J. Appl. Phys.* **43** (1972) 3943.
[4] Yu. M. Polukarov, Yu. D. Gamburg and M. I. Tcherepenina, in 'Issledovania po elektroosajdeniu i rastvoreniu metallov', Nauka, Moskow (1971) pp. 146–152.
[5] A. Gangulee, *J. Appl. Phys.* **45** (1974) 3749.
[6] D. S. Stoychev, I. V. Tomov and I. B. Vitanova, *J. Appl. Electrochem.* **15** (1985) 879.
[7] I. V. Tomov, D. S. Stoychev and I. B. Vitanova, *J. Appl. Electrochem.* **15** (1985) 887.
[8] M. B. Bever, D. L. Holt and A. L. Titchener, in 'Progress in Materials Science' (edited by B. Chalmers, J. W. Christian and T. B. Massalaki), Vol. 17, Pergamon Press, Oxford (1973).
[9] D. Lewis, D. O. Northwood and C. E. Pearce, *Corros. Sci.* **9** (1969) 787.
[10] J. S. Kallend and Y. C. Huang, *Metal Sci.* **18** (1984) 381.
[11] D. D. Sam and B. L. Adams, *Metall. Trans. A* **17A** (1986) 513.
[12] D. Stoychev, I. Vitanova, I. Pojarliev and S. Rashkov, *Poligraphia (Russ.)* **9** (1984) 37.
[13] L. G. Schulz, *J. Appl. Phys.* **20** (1949) 1033.
[14] H.-J. Bunge, 'Texture Analysis in Materials Science-Mathematical Methods' Butterworths, London (1982) p. 127.
[15] I. Tomov and H.-J. Bunge, *Texture Cryst. Sol.* **3** (1979) 73.
[16] R. Delhez, Th. H. de Keijser and E. J. Mittemeijer, *Fres. Z. Anal. Chem.* **312** (1982) 1.
[17] J. I. Langford, *J. Appl. Cryst.* **11** (1978) 10.
[18] Th. H. de Keijser, J. I. Langford, E. J. Mittemeijer and A. B. P. Vogels, *J. Appl. Cryst.* **15** (1982) 308.
[19] H. C. van de Hulst and J. J. M. Reesinck, *Astrophys. J.* **106** (1947) 121.
[20] E. A. Faulkner, *Phil. Mag.* **5** (1960) 519.
[21] M. Cook and T. L. Richards, *J. Inst. Metals* **70** (1944) 159.
[22] W. H. Baldwin, *Trans. AIME* **166** (1946) 591.
[23] H. Takechi, H. Kato and S. Nagashima, *Trans. AIME* **242** (1968) 56.
[24] M. Matsuo, S. Hayami and S. Nagashima, *Adv. X-ray Anal.* **14** (1971) 214.
[25] R. L. Every and M. Hatherly, *Texture* **1** (1974) 183.
[26] D. J. Willis and M. Hatherly, in 'Texture and the Properties of Materials', Metal Society, London (1976) p. 48.
[27] J. L. Lebrun, G. E. Maeder and P. Parmiere, 'Fifth Int. Conf. Texture of Materials' (edited by G. Gottstein and K. Lucke), Springer, Berlin (1978) Vol. II, p. 513.
[28] P. Ramarao and T. R. Anantharaman, *Trans. Ind. Inst. Metals* **18** (1965) 181.